mathematics

MDPI

Article

A Stochastic Weather Model for Drought Derivatives in Arid Regions: A Case Study in Qatar

Jayeong Paek †, Marco Pollanen * and Kenzu Abdella

Department of Mathematics, Trent University, Peterborough, ON K9L 0G2, Canada
* Correspondence: marcopollanen@trentu.ca
† Current address: Department of Statistics, Chonnam National University, Gwangju 61186, Republic of Korea.

Abstract: In this paper, we propose a stochastic weather model consisting of temperature, humidity, and precipitation, which is used to calculate a reconnaissance drought index (*RDI*) in Qatar. The temperature and humidity models include stochastic differential equations and utilize an adjusted Ornstein–Uhlenbeck (O–U) process. For the precipitation model, a first-order Markov chain is used to differentiate between wet and dry days and the precipitation amount on wet days is determined by a probability distribution. Five different probability distributions were statistically tested to obtain an appropriate precipitation amount. The evapotranspiration used in the *RDI* calculation incorporates crop coefficient values, depends on the growth stages of the crops, and provides a crop-specific and more realistic representation of the drought conditions. Five different evapotranspiration formulations were investigated in order to obtain the most accurate *RDI* values. The calculated *RDI* was used to assess the intensity of drought in Doha, Qatar, and could be used for the pricing of financial drought derivatives, a form of weather derivative. These derivatives could be used by agricultural producers to hedge against the economic effects of droughts.

Keywords: stochastic differential equations (SDEs); reconnaissance drought index (*RDI*); Ornstein–Uhlenbeck (O–U) processes; Markov chains

MSC: 65C30; 00A69; 00A72

Citation: Paek, J.; Pollanen, M.; Abdella, K. A Stochastic Weather Model for Drought Derivatives in Arid Regions: A Case Study in Qatar. *Mathematics* **2023**, *11*, 1628. https://doi.org/10.3390/math11071628

Academic Editors: Christos Floros, Christos Kountzakis and Konstantinos Gkillas

Received: 31 January 2023
Revised: 24 March 2023
Accepted: 24 March 2023
Published: 28 March 2023

1. Introduction

The motivation for this paper was to develop stochastic weather models to simulate weather for use in pricing financial drought derivatives [1], which are a form of weather derivative designed to protect agricultural producers from the economic effects of drought. In recent years, weather derivatives have become popular and effective tools for minimizing financial losses associated with weather impacts in many industries including energy, transportation, and agriculture. Before the use of weather derivatives, the most common approach to reducing weather risks was the use of insurance contracts. As insurance contracts are designed to pay out for specific weather events, which are mentioned in the contracts, they are effective only when these events occur. Usually, the events are likely disasters, such as typhoons or floods, which happen with low probability but cause big losses. However, weather insurance is plagued by moral hazards, as it may not incentivize policyholders to mitigate damages. Additionally, due to the potential for the high positive spatial correlation of claims, it can be difficult for insurers to meet their obligations. Due to the limitations of insurance contracts and the high variability of weather, weather derivatives are becoming more popular than insurance contracts for hedging weather risks [2].

Weather derivatives are similar to traditional derivatives on financial assets, but as their values are based on weather indices, there is no underlying traded asset to hedge against. This means that risk-neutral pricing models cannot be applied. Thus, the main approach to pricing them is to use Monte Carlo simulation. However, this presents difficulties due to limited

quantities of historical data. There are three Monte Carlo approaches to modeling the price of weather derivatives: historical burn analysis (HBA), index modeling, and daily modeling.

HBA, which is a classical method, uses historical price data to simulate future prices with the assumption that historical weather data contain all characteristics to value future prices of derivatives [3]. Therefore, we need to have the price of weather derivatives to employ HBA. Instead, there is an approach to model index values that are directly related to the price of weather derivatives. In this approach, a different model is required for each index [4]. Another approach suggested by recent studies is daily modeling. We use weather models that can simulate potential future weather data. This approach can lead to more accurate results compared to the other two approaches because it utilizes weather data directly to price weather derivatives [5].

Literature on weather derivatives has primarily focused on alternative models for pricing weather risks [6–9]. However, while weather derivatives are often used to protect agricultural producers from droughts, there is a basis risk in that weather does not perfectly correlate with drought risks. Thus, our interest is to improve the use of stochastic weather models to simulate drought indices, enabling the pricing of drought-specific derivatives to better capture potential risks. Furthermore, in the literature, studies have not focused on weather modeling in arid climates, where droughts are prevalent. Thus, in this paper, we assess our stochastic weather models by calculating a reconnaissance drought index (*RDI*) in Qatar for use in index-based weather derivatives. Modeling weather to calculate *RDI* provides not only an opportunity to price drought derivatives but also could be used to potentially understand the distribution of losses in traditional drought insurance contracts, thus providing more accurate pricing.

Developing stochastic models to simulate realistic daily weather scenarios that preserve the statistical characteristics of the historical weather data is very important to obtain accurate prices of weather derivatives [2]. In this study, based on daily modeling, we suggest stochastic weather models for temperature, humidity, and precipitation to decide the prices of weather derivatives.

When it comes to discrete temperature modeling, an autoregressive (AR) model for residuals was used to model daily temperature [10] as a discrete process. As an improved autoregressive model, reference [11] suggested a k-lag autocorrelation model. The continuous processes for temperature models usually contain a mean-reverting term. Most of the temperature models suggested for weather derivatives consider a mean-reverting process. Reference [12] uses an O–U process for the temperature at Heathrow Airport in the UK and concludes that it shows a good fit for modeling temperature. The study in [12] proposes an adjusted O–U process pointing out the problem that the expected value of the O–U process suggested in [13,14] does not approximately equal the mean that the process should approach. In an early study of precipitation models, Reference [15,16] suggested a Markov chain for modeling of precipitation occurrence. A first-order Markov chain is a well-known and widely used model for precipitation occurrence [17–19]. A higher-order Markov chain is also applied to model precipitation occurrence to overcome the problem of the short memory length found in a first-order Markov chain model [20,21]. A Markov chain model with jumps for precipitation data in Chongqing, China shows better results for locations with frequent excess precipitation [22].

This paper is structured as follows. In Section 2, we describe the reconnaissance drought index (*RDI*) as a measure of drought intensity, evapotranspiration, and crop evapotranspiration used to calculate drought index values; we also propose stochastic weather models for temperature, humidity, and precipitation. In Section 3, we calculate the *RDI* values for four crops in Qatar, i.e., carrots, maize, tomatoes, and wheat, using historical and simulated weather data. In Section 4, we discuss our conclusions and future work.

2. Materials and Methods

2.1. Study Area and Data

In this study, daily weather data from Doha, Qatar is used. Qatar is located at latitude 25.35° N and longitude 51.03° E, in the eastern region of Saudi Arabia. It has a dry climate with low precipitation and exceedingly hot and humid summers. The temperature during the winter months, from December to February, remains above 10 °C and most of the precipitation occurs during this period. The region receives a small amount of precipitation, as shown in Figure 1, which is highly unpredictable both in terms of time and space.

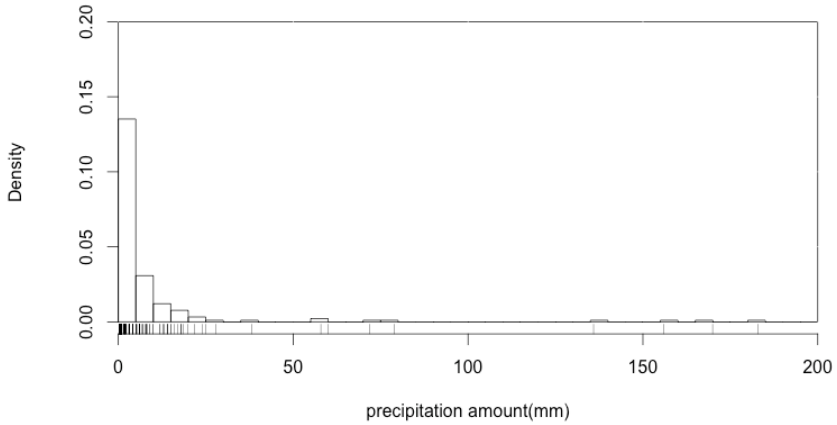

Figure 1. Histogram of precipitation amount in Doha (mm).

Weather data from 1983 to 2013 were used to develop a stochastic weather model. To compare calculation methods for evapotranspiration, data over the period from 1985 to 2013 were used. The data included basic weather factors, such as daily values of the mean, minimum, and maximum temperature (°C), precipitation (mm), relative humidity (%), and wind speed (m/s). More detailed weather factors for calculating evapotranspiration were included from 1985.

To ignore the effects of leap years, we subtract the last day (i.e., 29 February) in a leap year. This gives us a simple model structure with an equal number of days in each year, with 365 days in every year.

In this study, missing values in the temperature data were replaced with the existing values of the same day in the previous year. This is because missing values found in our data were mostly consecutive and over a long period; for example, the worst case is that there were no data for the whole month. For precipitation, missing data values were considered as non-rainy days because in Qatar there were not many rainy days. All data processing and calculations were done with the statistical software package R.

2.2. Reconnaissance Drought Index (RDI)

In the last few decades, many drought indices have been developed as tools for assessing the severity of droughts. By incorporating the effects of relevant weather variables on the occurrence and intensity of droughts into a single numerical value, drought indices make it easy to establish strategies that could reduce the associated risks. Through the drought index, droughts could be classified as hyper-arid, arid, semi-arid, sub-humid, and humid. In this paper, we used a more recent drought index called the reconnaissance drought index (*RDI*), introduced by Tsakiris et al. (2007) [23]. The *RDI* is a physically based, universal, and comprehensive index that depends on cumulative precipitation and potential evapotranspiration. Most drought indices are precipitation-based only and are not sufficiently effective at capturing the effects of droughts on crops and agricultural production. When assessing the severity of droughts, evapotranspiration is also required in order to provide the most realistic information on water scarcity and agricultural conditions. Therefore, the *RDI* is a preferred index for use in agriculture in drought severity assessment

and monitoring. It is also sensitive to changing climatic environments and flexible for different growing periods (Tsakiris et al. (2007) [23]).

RDI is defined as the ratio of accumulated precipitation to potential evapotranspiration [23]:

$$RDI^i = \frac{\sum_{j=1}^{n} P_{ij}}{\sum_{j=1}^{n} PET_{ij}}, \quad (1)$$

where P_{ij} and PET_{ij} are the precipitation and potential evapotranspiration (PET) for the jth month of the ith year and n is the period in which we are interested. Based on this equation, we can calculate *RDI* for any period in each year. Potential evapotranspiration (PET) is the evaporation that occurs where there is a sufficient water supply, but in practice it is very hard to obtain. Therefore, in practice, we use an adjusted *RDI*, which uses actual evapotranspiration (ET) instead of potential evapotranspiration (PET):

$$RDI^i_{adj} = \frac{\sum_{j=1}^{n} P_{ij}}{\sum_{j=1}^{n} ET_{ij}}, \quad (2)$$

where ET_{ij} is the actual evapotranspiration ET for the jth month of the ith year.

2.3. Evapotranspiration

Evapotranspiration consists of two processes that account for water loss to the atmosphere: evaporation and transpiration. While evaporation represents the water loss due to movement from the soil to the atmosphere, transpiration represents the water loss through plants. Since these two processes occur simultaneously, it is difficult to measure their effect separately. Therefore, we use evapotranspiration as a quantity that measures the combined effect of the two processes. Since the weather is the only factor that affects evapotranspiration, there are calculation methods using weather data. Several calculation methods have been developed and proposed to estimate evapotranspiration from weather data such as temperature, humidity, wind speed, and other weather parameters, such as solar radiation, pressure, and so on.

The FAO-56 Penman–Monteith (PM) method [24] is recommended by the Food and Agriculture Organization of the United Nations (FAO) as a standardized method to calculate the reference evapotranspiration ET_0. It has the following form:

$$ET_0 = \frac{0.408\Delta(R_n - G) + \gamma\left[\frac{900}{(T+273)}U_2(e_s - e_a)\right]}{\Delta + \gamma(1 + 0.34U_2)}, \quad (3)$$

where ET_0 is the reference evapotranspiration (mm/day), R_n is the net radiation at the crop surface (MJ/m^{2}day), G is the soil heat flux density (MJ/m^{2}day), T_2 is the mean air temperature at a 2 m height (°C), U_2 is the wind speed at a 2 m height (m/s), e_s is the saturation vapor pressure (kPa), e_a is the actual vapor pressure (kPa), Δ is the slope of the vapor pressure curve (kPa/°C), and γ is a psychometric constant (kPa/°C).

The limitation of using the PM formulation is that it requires extensive climatic data that are not easily available. Therefore, we test other simpler evapotranspiration formulations for compatibility with the PM formulation for Qatar, including those developed by Blaney and Criddle [25], Hargreaves and Samani [26], Jensen and Haise [27], Linacre [28], and Turc [29]. This will be crucial for other arid regions where the available weather data are limited. The formulations of each of these methods are provided in Appendix A.

In order to select the appropriate formulation, we compared the compatibility of each of these methods with the PM formulation by computing various statistical quantities, including, the Pearson's correlation (R^2), root-mean-square error (RMSE), mean absolute error (MAE), and the maximum absolute error (MAXE). The computed values of these quantities based on the data from 1985 to 2014 are presented in Table 1.

Table 1. Statistics for the comparison of ET_0 methods.

	Blaney and Criddle	Hargreaves and Samani	Jensen and Haise	Lincare	Turc
R^2	0.5107	0.7283	0.5765	0.4367	0.7623
RMSE	2.8507	1.6317	2.4806	10.3425	1.4817
MAE	2.4389	1.3574	2.1244	8.9496	1.2232
MAXE	5.636	3.8584	5.8988	24.0355	3.4935

With the highest correlation R^2 value and lowest RMSE, MAE, and MAXE error values, the Turc method shows the closest agreement with the PM method. The Turc method is given by the following piecewise continuous function or relative humidity RH

$$\begin{aligned} ET_0 &= 0.013\left(\frac{T_{mean}}{15+T_{mean}}\right)(R_s+50), \qquad RH > 50\% \\ &= 0.013\left(\frac{T_{mean}}{15+T_{mean}}\right)(R_s+50)\left(1+\frac{50-RH}{70}\right), \qquad RH < 50\%, \end{aligned} \tag{4}$$

and requires only mean temperature, T_{mean} (ºC), relative humidity, RH (%), and mean solar radiation, R_s (W/m^{2}day), which are variables that are easily obtainable over an arid region, such as Qatar, making the method suitable for common use. Therefore, the Turc method is selected as a method of evapotranspiration for the RDI calculation in this paper.

Once we obtain ET_0, the actual evapotranspiration specific to a certain crop can be easily calculated using the crop coefficient. While most of the effects from relevant weather conditions are reflected in ET_0, the effect of the crop type on evapotranspiration is incorporated by adjusting ET_0 with the crop coefficient to obtain the crop evapotranspiration, denoted by ET_c, which is given by:

$$ET_c = ET_0 \times k_c\,, \tag{5}$$

where k_c is the crop coefficient. Every crop has its own crop coefficient values based on the growth environment, water requirements, and growth stages. Crop coefficients for specific crops at specific growth stages are provided by the Food and Agriculture Organization of the United Nations (FAO) [24]. Table 2 shows the growth period and crop coefficients for Qatar. The growth period is separated into four growth stages; initial, development, mid-season, and late season. Typically, crop coefficients in mid-season have the largest values. Most crops in Qatar are grown in the winter months and harvested before the start of the summer months because the summer has very few rainy days.

Crop evapotranspiration for six crops, including alfalfa, bean, carrot, maize, tomato, and wheat, was calculated using observed and simulated weather data. Observed weather data from 1985 to 2013 and simulation data with the same length as the observation data were used. The mean, standard deviation, minimum, and maximum of crop evapotranspiration are presented in Table 3. The mean crop evapotranspiration from tomatoes shows the largest value, while alfalfa shows the smallest value.

Table 2. Growing periods and crop coefficients in Qatar (FAO 56, 1988).

Crop	Growing Period		Growth Stage				k_c (Crop Coefficient)		
	Planting	Harvest	Initial	Dev	Mid	Late	Initial	Mid	Late
Alfalfa	1-Jan	2-Mar	10	20	20	10	0.40	0.95	0.40
Bean	15-Sep	29-Nov	15	25	25	10	0.50	1.15	0.90
Carrot	15-Oct	12-Feb	20	30	50	20	0.70	1.05	0.95
Cucumber	15-Nov	25-Mar	25	35	50	20	0.60	1.00	0.75
Maize	1-Jan	21-May	25	40	45	30	0.30	1.20	0.60
Onion	15-Oct	31-May	20	35	110	45	0.70	1.05	0.75
Potato	1-Dec	20-Apr	30	35	50	25	0.50	1.15	0.75
Rice	1-Dec	30-Apr	30	30	60	30	1.05	1.20	0.70
Tomato	1-Jan	16-May	30	40	40	25	0.60	1.15	0.80
Wheat	15-Dec	24-May	20	50	60	30	0.70	1.15	0.30

Table 3. Summary statistics of ET_c.

Crop	Observation				Simulation			
	Mean	SD	Min	Max	Mean	SD	Min	Max
Alfalfa	1.6790	0.6127	0.3651	3.4470	1.1920	0.4732	0.2531	2.6430
Bean	2.6640	0.6936	0.7510	4.6270	2.0430	0.5325	0.8086	3.7270
Carrot	2.1840	0.3488	0.9584	3.8760	1.5560	0.3148	0.5188	2.9350
Maize	2.7510	1.2636	0.2738	6.4760	2.4020	1.2528	0.1638	6.3320
Tomato	2.8830	1.0954	0.5477	6.2060	2.5150	1.2096	0.3277	6.0680
Wheat	2.5730	1.1111	0.6206	6.2060	2.1510	1.1037	0.4033	6.0680

2.4. Temperature Model

We propose using the mean reversion process to develop the temperature model accounting for its seasonality, which repeats annually. We use an adjusted Ornstein–Uhlenbeck (O–U), suggested by [13,14] and given by

$$dX_t = \left[\lambda(\mu - X_t) + \frac{d\mu}{dt}\right]dt + \gamma dW_t\,, \tag{6}$$

where X_t represents the daily temperature, λ is the speed of mean reversion, μ is the mean where the process reverts to, γ is the volatility of the model, and dW_t is the Wiener process, which is normally distributed with a mean of 0 and variance of t. The solution to Equation (6), a stochastic differential equation (SDE), is derived from Itô's Lemma and is given by [13]:

$$X_t = \mu - e^{-\int_0^t \lambda\, ds}(\mu + X_0) + e^{-\int_0^t \lambda\, ds}\int_0^t e^{-\int_0^t \lambda\, ds}\gamma dW_s\,. \tag{7}$$

In this process, λ, μ, and γ are parameters that need to be estimated from the data. Here, we use the least-squares method to estimate these parameters, where we assume that consecutive observations have a linear relation with normally distributed error. The following linear equation is applied to the solution of the SDE [30]:

$$X_t = a + bX_{t-1} + \epsilon\,. \tag{8}$$

The relationship between the parameters of the linear equation and the solution of the SDE [30] is then derived and described below.

$$a = \mu\left(1 - e^{-\lambda\delta}\right), \tag{9}$$

$$b = e^{-\lambda\delta}, \tag{10}$$

and,

$$sd(\epsilon) = \gamma\sqrt{\frac{1-e^{-2\lambda\delta}}{2\lambda}}. \tag{11}$$

Here, δ represents the time step between t and $t-1$, so δ is 1. Thus, rewriting with respect to parameters in the SDE, we have

$$\lambda = -\frac{\ln b}{\delta}, \tag{12}$$

$$\mu = \frac{a}{1-b}, \tag{13}$$

and,

$$\gamma = sd(\epsilon)\sqrt{\frac{-2\ln b}{\delta(1-b^2)}}. \tag{14}$$

We can calculate the parameters of the least square fit as follows:

$$a = \frac{S_y - bS_x}{n}, \tag{15}$$

$$b = \frac{nS_{xy} - S_xS_y}{nS_{xx} - {S_x}^2}, \tag{16}$$

$$sd(\epsilon) = \sqrt{\frac{nS_{yy} - {S_y}^2 - b(nS_{xy} - S_xS_y)}{n(n-2)}}, \tag{17}$$

where $S_x = \sum_{t=1}^{n} X_{t-1}$, $S_y = \sum_{t=1}^{n} X_t$, $S_{xx} = \sum_{t=1}^{n} X_{t-1}^2$, $S_{xy} = \sum_{t=1}^{n} X_{t-1}X_t$ and $S_{yy} = \sum_{t=1}^{n} X_t^2$.

The mean values of the parameters in the SDE are calculated for each month of the year and are presented in Table 4. The highest value of γ is found in June and the smallest value is found in October. For a speed of mean reversion, August has a large value of λ, which means it is drawn very strongly back to its mean value. Moreover, the value of μ is close to the monthly mean temperature.

Table 4. Parameter values of the mean reversion process for the temperature.

Month	μ	λ	γ
January	17.4780	0.4011	1.6294
February	18.8917	0.4824	1.7278
March	22.3762	0.4331	1.7986
April	28.2374	0.2821	1.5822
May	33.1215	0.3567	1.6389
June	35.0124	0.6396	1.9190
July	35.7646	0.6965	1.8501
August	35.1229	0.9300	1.5149
September	32.8898	0.5524	1.2789
October	28.6960	0.2412	0.8825
November	23.7035	0.1493	1.1662
December	18.8716	0.3034	1.4249

We also used the maximum likelihood estimation method to estimate these parameters and very similar results were obtained. (See Appendix B for details).

2.5. Humidity Model

In addition to temperature, relative humidity is needed to calculate evapotranspiration using our selected Turc method. Similar to the temperature model, a mean-reverting O–

U process is used to model daily humidity data. The SDE equation given by Equation (6) and its solution given by Equation (7) are applied, where X_t represents humidity. The parameters are then determined using Equations (12)–(14). The mean values of the parameters in the SDE were calculated using the least square method for each month of the year and are presented in Table 5. Similar results were obtained using the maximum likelihood estimation method (see Appendix B for details). As one may expect, the volatility values for humidity are larger than those for the temperature model.

Table 5. Parameter values of the mean reversion process for humidity.

Month	μ	λ	γ
January	67.4488	0.6768	11.4293
February	64.0371	0.9049	14.8098
March	54.9218	0.7767	15.1913
April	46.4332	0.5920	12.7813
May	36.3553	0.7387	12.2807
June	35.3932	0.7081	14.4253
July	45.2631	0.5689	15.4916
August	55.2619	0.7355	14.2856
September	56.2345	1.1614	15.9156
October	58.7774	0.9829	11.9194
November	62.1151	1.1193	11.0523
December	67.9820	0.8075	10.6235

2.6. Precipitation Model

We now present the precipitation model, which is required along with evapotranspiration for *RDI* calculation.

The most commonly used stochastic models for precipitation consist of a two-process formulation that models precipitation occurrence and amount. In the two-process model, a Markov chain is used to model precipitation occurrence, and a probability distribution is used to determine the precipitation amount on a wet day [15–19,31,32]. In the following sections, we describe the first-order Markov chains used to model precipitation occurrence and consider several probability distributions for estimating the precipitation amount.

2.6.1. Precipitation Occurrence Model

The first-order Markov chain implicitly assumes that the probability of rain tomorrow depends only on whether it rained today or not and is described by the Markov property:

$$P(X_{t+1} = s_{t+1} | X_t = s_t, X_{t-1} = s_{t-1}, \cdots, X_0 = s_0) = P(X_{t+1} = s_{t+1} | X_t = s_t), \quad (18)$$

where time $t = \{0, 1, 2, \cdots, T\}$ and state space $s = \{1, 2, 3, \cdots, S\}$. The Markov chain transition matrix that defines a probability that each event occurs is composed of transition probabilities, which are conditional probabilities of future state j given state i. The transition matrix, denoted by $\mathbf{P}$, is given by

$$\mathbf{P} = \begin{bmatrix} p_{11} & \cdots & p_{1j} \\ \vdots & \ddots & \vdots \\ p_{i1} & \cdots & p_{ij} \end{bmatrix} \quad \text{for } i, j \in S, \quad (19)$$

where $p_{ij} = P(X_{t+1} = j | X_t = i)$. The property of a transition matrix is that the total sum of each row must equal 1, i.e.,

$$\sum_{j=1}^{S} p_{ij} = \sum_{j=1}^{S} P(X_{t+1} = j | X_t = i) = 1. \quad (20)$$

The precipitation occurrence has two states: dry and wet. Therefore, the transition matrix is specified by two conditional probabilities, which are

$$p_{dd} = P(\text{dry on day t+1}|\text{dry on day t}), \tag{21}$$

$$p_{dw} = P(\text{wet on day t+1}|\text{dry on day t}), \tag{22}$$

$$p_{wd} = P(\text{dry on day t+1}|\text{wet on day t}), \tag{23}$$

$$p_{ww} = P(\text{wet on day t+1}|\text{wet on day t}). \tag{24}$$

Since there are only two states, transition probabilities at the same given state are complementary. So it is not necessary to estimate four transition probabilities, we only need to estimate one of each pair of transition probabilities. For instance, the probability of a dry day following a dry day is calculated using the probability of a wet day following the dry day, which is $p_{dd} = 1 - p_{dw}$. The probability transition matrix is defined as below.

$$\mathbf{P} = \begin{bmatrix} p_{dd} & p_{dw} \\ p_{wd} & p_{ww} \end{bmatrix} \qquad 0 \leq p_{ij} \leq 1 \qquad i, j = \{d, w\}. \tag{25}$$

Using the transition matrix, we can calculate the stationary state vector such that $\boldsymbol{\pi} = \boldsymbol{\pi}\mathbf{P}$. It implies a long-run relative frequency of precipitation occurrence and satisfies $\sum_{i=1}^{S} \pi_i = 1$, where $\pi_i \geq 0$ for all i. Each element, π_i, denotes the probability of being in state i. If this state vector is given by

$$\boldsymbol{\pi} = \begin{pmatrix} \pi_d & \pi_w \end{pmatrix}, \tag{26}$$

then it must satisfy

$$\begin{pmatrix} \pi_d & \pi_w \end{pmatrix} = \begin{pmatrix} \pi_d & \pi_w \end{pmatrix} \begin{bmatrix} 1 - p_{dw} & p_{dw} \\ p_{wd} & 1 - p_{wd} \end{bmatrix}. \tag{27}$$

Therefore, by solving the stationary probabilities π_d and π_w, we obtain:

$$\pi_d = \frac{p_{wd}}{p_{wd} + p_{dw}}, \tag{28}$$

$$\pi_w = \frac{p_{dw}}{p_{wd} + p_{dw}}. \tag{29}$$

The stationary probabilities are calculated for each month and are shown in Table 6. We can see that most of the stationary probabilities for dry days are quite large, showing that Qatar does not have many wet days. Since there are no wet days in June and July from the data, stationary probabilities for dry days are one, as expected.

Table 6. Steady-state probability vectors for precipitation occurrence in Doha.

Month	Probability Vector	Month	Probability Vector
January	[0.965 0.035]	July	[1 0]
February	[0.971 0.029]	August	[0.999 0.001]
March	[0.97 0.030]	September	[0.999 0.001]
April	[0.976 0.024]	October	[0.998 0.002]
May	[0.993 0.007]	November	[0.976 0.024]
June	[1 0]	December	[0.960 0.040]

2.6.2. Distribution of Precipitation Amount

By accounting for the fact that there is an extreme amount of precipitation over 100 mm, we expect that distributions with thicker tails will perform better in estimating the precipitation amount. Therefore, we employed two extreme distributions, the generalized extreme value, and four-kappa distributions. Since these distributions have thicker tails, they can better capture extremely large amounts of precipitation in the simulation.

In this study, we also considered the probability distributions used in previous research, including the exponential, log-normal, and gamma distributions, and two extreme distributions, i.e., the general extreme value and four-kappa distributions, to simulate the precipitation amount. The parameters of these distributions are estimated using the maximum likelihood method (MLE), which is the most common method used to find parameters in statistics.

Once we have the precipitation occurrence sequence, the next step is to determine the precipitation amounts on wet days. Since the precipitation amount is generally small, we use a right-skewed probability distribution for the precipitation amount [19]. Previously, many right-skewed probability distributions, including the exponential, log-normal, and gamma, were used to describe the distribution of the precipitation amount [18,33]. In this study, we consider exponential, log-normal, and gamma distributions, and two extreme probability distributions, the general extreme value distribution (GEVD) and four-kappa distribution (K4D). Functions for the probability distributions are given in Table 7. The two extreme distributions have a thick tail, which could model the extreme amount of precipitation in the simulation. The probability distribution parameters are estimated using the maximum likelihood estimation (MLE), and the results are shown in Table 8.

Table 7. Functions for the probability distributions.

Distribution	
Exponential (density)	$f(x;\lambda) = \lambda \exp(-\lambda x), \quad x \geq 0;\ \lambda > 0$
Log-normal (density)	$f(x;\mu,\sigma) = \frac{1}{x\sigma\sqrt{2\pi}} \exp\left(\frac{-(\ln x-\mu)^2}{2\sigma^2}\right), \quad x > 0;\ \sigma > 0$
Gamma (density)	$f(x;\alpha,\beta) = \frac{\beta^{-\alpha} x^{\alpha-1} e^{-x/\beta}}{\Gamma(\alpha)}, \quad x > 0;\ \alpha,\ \beta > 0$
GEVD (CDF)	$F(x;\xi,\mu,\alpha) = \exp\left\{-\left[1+\xi\left(\frac{x-\mu}{\alpha}\right)\right]^{-1/\xi}\right\},$ where $x \in \{z \mid 1+\xi(z-\mu)/\alpha > 0\};\ \sigma > 0$
K4D (CDF)	$F(x;\xi,\alpha,h,k) = \left[1-h\left[1-\frac{k(x-\xi)}{\alpha}\right]^{\frac{1}{k}}\right]^{\frac{1}{h}}, \quad k \neq 0,\ h \neq 0$ (See [34] for a description of the support of K4D.)

Table 8. Estimation of parameters in probability distributions.

Distribution	**Estimation of Parameters**			
Exponential	$\hat{\mu} = 0.108$			
Log-normal	$\hat{\mu} = 0.834$	$\hat{\sigma} = 1.510$		
Gamma	$\hat{\alpha} = 0.463$	$\hat{\beta} = 0.050$		
GEVD	$\hat{\mu} = 1.060$	$\hat{\alpha} = 1.322$	$\hat{\xi} = 1.364$	
K4D	$\hat{\xi} = 1.225$	$\hat{\alpha} = 1.424$	$\hat{h} = -0.375$	$\hat{k} = -1.329$

It would be preferable to fit probability distributions for each month. However, some months have very few or no rainy days in our data, making it challenging to find suitable

probability distributions. Therefore, we use all the available precipitation data to estimate the probability distribution of precipitation amount in Qatar.

We determine which probability distributions show the best fit for the precipitation amount by using three model validation methods, the Kolmogorov–Smirnov (KS test), Akaike information criteria (AIC), and Bayesian information criteria (BIC). As described below, the KS test provides p-values while both AIC and BIC provide values based on likelihood functions [33].

1. Kolmogorov–Smirnov test (KS test [33])
   The Kolmogorov–Smirnov test is used to determine if a dataset comes from a specified distribution. It measures the differences between the empirical distribution of the sample and the cumulative distribution of the specified distribution, providing a test statistic, D, and p-values that can be used as criteria for hypothesis testing.
2. Akaike information criteria (AIC [35])
   Firstly, the AIC developed by Hirotugu Akaike was used to evaluate the performance of the model in a simple linear regression. It was created to select the model that has the smallest loss of information from the given data. It measures the loss based on a likelihood function and is defined by:

$$AIC = -2\ln(L) + 2K, \tag{30}$$

   where L is the likelihood function and K is the number of parameters. In the formula, the negative log-likelihood term represents the loss of information and $2K$ contains a penalty corresponding to the number of parameters in the model. This penalty considers the number of parameters because the model performance improves with the number of parameters it has. By comparing AIC, the model with the smallest AIC is considered to have good performance.
3. Bayesian information criterion (BIC [36])
   Similar to AIC, BIC evaluates the model performance by using the likelihood, and the model with the smallest BIC is preferred. Compared to AIC, it has a larger penalty term for the number of parameters and observations. It is defined by

$$BIC = -2\ln(L) + K\ln(n). \tag{31}$$

The results of the KS test, AIC, and BIC for all of the distributions are presented in Table 9.

Table 9. Results of the KS test, AIC, and BIC.

Distribution	KS Test (p-Value)	AIC	BIC
Exponential	2.2×10^{-16}	1174.589	1177.793
Log-normal	9.937×10^{-4}	973.921	980.329
Gamma	1.467×10^{-6}	1075.677	1082.085
GEVD	1.467×10^{-6}	953.895	963.507
K4D	0.0929	999.214	1008.03

The p-values of all distributions except K4D are very small and much less than the significance level of 0.05, indicating that only K4D is a significant distribution resulting from the KS test. Furthermore, since the AIC and BIC values of K4D are among the smaller values, we choose to adopt the K4D distribution for the amount of precipitation on wet days.

3. Results

We use the solution of the SDE to simulate daily temperatures and compare them with the observed temperature data. Summary statistics of the observation and simulation data are summarized in Table 10. The mean daily temperature from observation, 27.67, is consistent with the simulation result of 27.57. Standard deviations from observation and

simulation data are 6.8975 and 6.9036, respectively, which are close to each other. Additionally, the 1st, 10th, 25th, 50th, 75th, 90th, and 99th percentiles show similar consistencies. Therefore, the temperature model with the adjusted O–U process is able to adequately reproduce the properties of temperature found in the observation.

Table 10. Comparison of the summary statistics of the temperature (°C).

Statistics	**Observation**	**Simulation**
Mean	27.67	27.57
SD	6.89756	6.903637
Min	9.80	11.48
Max	42.20	41.78
Percentile	Observation	Simulation
1	14.22	14.99241
10	17.90	17.95062
25	21.40	20.99015
50	28.70	28.54294
75	33.90	34.00301
90	35.90	35.83885
99	38.60	38.14206

Similarly, the summary statistics for the SDE simulation are presented in Table 11. The mean humidity of the simulation is very close to the observation. In addition, percentiles in the simulation are very similar to each other. The humidity simulation shows a smaller standard deviation than the observation. The main discrepancy is found in the minimum values. The minimum observation humidity is 8 but the simulation minimum is 2.252. Overall, the performance of the humidity model with the mean reverting O–U process is adequate.

Table 11. Comparison of the summary statistics of humidity (%).

Statistics	**Observation**	**Simulation**
Mean	54.01	54.210
SD	16.2691	14.92881
Min	8.00	2.252
Max	95.00	98.900
Percentile	Observation	Simulation
1	18.00	17.39385
10	30.00	33.39348
25	42.00	44.32667
50	56.00	55.76611
75	66.00	64.95842
90	74.00	72.4125
99	85.00	83.9390

In terms of precipitation, 30 years of simulation data were generated using the stochastic precipitation model with a Markov chain. The number of wet days in the observed and simulated data is presented in Figure 2. The number of wet days in the observed and simulated data is very similar, indicating that a first-order Markov chain works well to generate precipitation occurrence. From the simulation data, the number of wet days in January, March, and August is generated more than in the observed data. The simulated number of wet days in February, April, May, October, November, and December is generally less than the observed data.

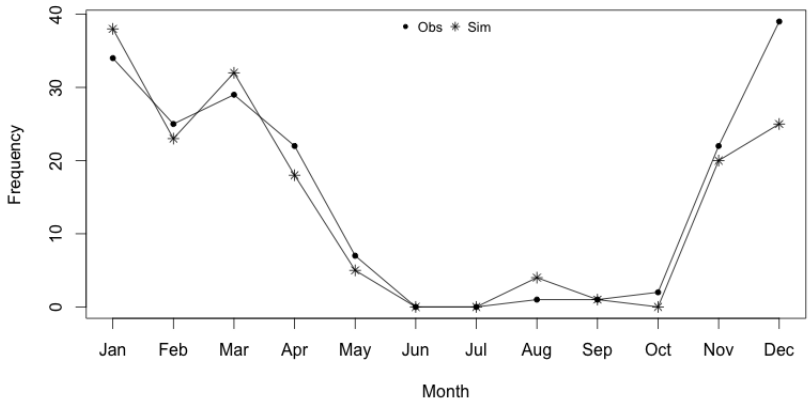

Figure 2. Comparison of rainy days from the observation and simulation data.

In order to compare the precipitation amounts between observation and simulation data, percentiles and means are calculated using the selected probability density K4D. The minimum, 25th percentile (Q1), median (Q2), mean, 75th percentile (Q3), and the maximum simulated precipitation data are presented in Table 12. It is evident that a right-skewed distribution is appropriate for the distribution of precipitation amount since the median of the observed precipitation amount is smaller than the mean. Most of the simulated percentiles are very similar to those from the observation data.

Table 12. Comparison of observation and simulation precipitation data.

	Observation	Simulation 2 (K4D)
Minimum	0.25	0.19
Q1	0.76	0.67
Q2 (Median)	1.78	1.53
Mean	9.22	8.68
Q3	6.10	4.71
Maximum	182.88	186.04

Figure 3 illustrates the histogram of the precipitation amounts obtained with K4D. The dashed line represents the simulation and both the data and the simulation clearly show that the distribution of precipitation amount is strongly rightly skewed.

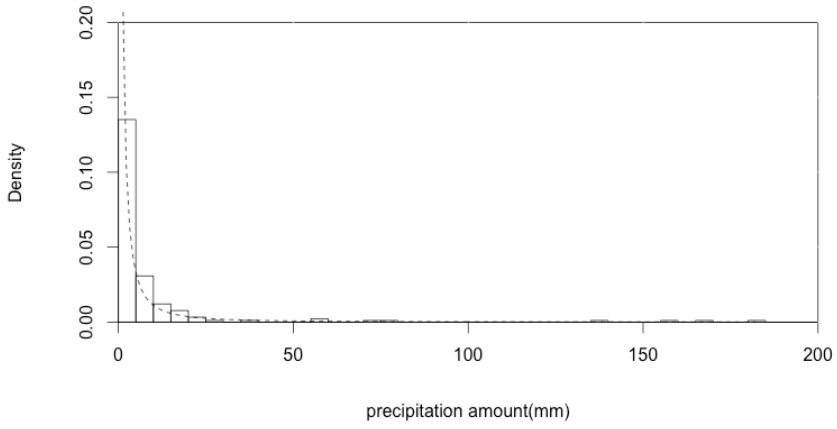

Figure 3. Comparison of the precipitation histogram and K4D.

We can calculate *RDI* using the observed and simulated weather data. To obtain simulation data, temperature and humidity data are simulated from an adjusted O–U process and precipitation data are simulated using a first-order Markov chain with K4D. *RDI* values for four crops—carrots, maize, tomatoes, and wheat—where calculated. Mean, standard deviation, and maximum values are presented in Table 13. No minimum values are presented here since all of the crops considered yield a minimum value of 0.

Table 13. Summary statistics of *RDI* in Doha.

Crop	Observation			Simulation		
	Mean	SD	Max	Mean	SD	Max
Carrot	0.1268	0.1827	0.7161	0.1460	0.2133	0.7788
Maize	0.0700	0.1104	0.4678	0.1141	0.1827	0.7602
Tomato	0.0692	0.1093	0.4631	0.1130	0.1813	0.7567
Wheat	0.0799	0.1047	0.4303	0.1153	0.1823	0.7341

As expected, *RDI* in Qatar is very small, which implies that Qatar is very dry. It is hard to grow crops only relying on water from precipitation in Qatar. So it is absolutely necessary to utilize effective irrigation systems to grow crops in Qatar. From the observation data, the smallest mean value is found for tomatoes, while the largest mean value is found for carrots, which also has the largest standard deviation. When comparing the *RDI* from observation and simulation data, the mean values from the simulation are higher than those from observation. The common trend shown in the mean and maximum values is that the *RDI* from simulation is higher than that from observation data. From this perspective, we can conclude that the dryness contained in the simulation weather data is less than that from observation.

4. Discussion

We developed a stochastic weather model for temperature, humidity, and precipitation in Qatar. We used an adjusted O–U process to simulate temperature and humidity, while for the precipitation model, we employed a Markov chain with a probability distribution. A first-order Markov chain was used to determine whether a day was wet or dry, and K4D was used to determine the precipitation amount on wet days.

Moreover, we calculated *RDI* values from observation and simulated weather data and compared them by computing the mean, standard deviation, and maximum values. *RDI* from the observation is obviously small since Qatar is generally dry. The mean and maximum values of *RDI* from the simulation are greater than the observation. The comparison results between the observation and simulation tell us that the dryness included in the simulation data is less than in the observation.

To improve stochastic weather models and obtain better simulation data, we suggest a combined weather model. In this study, we constructed temperature and humidity models separately. In fact, humidity is somehow related to temperature, so we could develop a combined model with temperature and humidity. With a combined model, we expect to have simulation data that will likely be in better agreement with real data. Thus, we can reduce the differences in the drought index values between the observation data and simulation data.

Author Contributions: Conceptualization, M.P. and K.A.; methodology, J.P. and M.P.; software, J.P.; validation, J.P.; investigation, J.P.; resources, K.A.; data curation, J.P.; writing—–original draft preparation, J.P.; writing—review and editing, M.P.; supervision, M.P. and K.A.; project administration, K.A.; funding acquisition, K.A. and M.P. All authors have read and agreed to the published version of the manuscript.

Funding: This publication was funded by NPRP grant no. NPRP6-064-4-001 from the Qatar National Research Fund (a member of the Qatar Foundation). The statements made herein are solely the responsibility of the authors.

Data Availability Statement: Publicly available datasets were analyzed in this study. This data can be found here: https://weatherspark.com/download/149641/Download-Hamad-International-Airport-Qatar-Weather-Data.

Conflicts of Interest: The authors declare no conflict of interest. The funders had no role in the design of the study; in the collection, analyses, or interpretation of data; in the writing of the manuscript, or in the decision to publish the results.

Appendix A. Evapotranspiration Formulations

In this Appendix, we provide the details of the formulations developed by Blaney and Criddle [25], Hargreaves and Samani [26], Jensen and Haise [27], Linacre [28], and Turc [29]. Each method has different data requirements; they are simpler equations and require fewer data variables compared to the FAO-56 PM method.

1. Blaney–Criddle:
   The Blaney–Criddle equation can be written as follows:

$$ET_0 = P(0.46T_{mean} + 8.13) \tag{A1}$$

   where T_{mean} is the mean temperature (°C) and P is the percentage of daylight hours associated with latitude and longitude.
2. Hargreaves:
   The Hargreaves equation can be written as follows:

$$ET_0 = 0.0023 \times R_a(T_{mean} + 17.80)\sqrt{T_{max} - T_{min}} \tag{A2}$$

   where T_{mean}, T_{max}, and T_{min} are the mean, maximum, and minimum temperatures (°C), respectively, and R_a is the extraterrestrial radiation (MJ/m^{2}day) computed from the latitude in radians, sunset hour angle, distance between the sun and Earth, and solar declination.
3. Jensen–Haise:
   The method developed by Jensen–Haise for the arid and semiarid regions has the following equation:

$$\begin{aligned} PET = & \frac{1}{38 - \left(2 \times \frac{Elevat}{305}\right) + 7.6\frac{50}{(e_{s(T_{max})} - e_{s(T_{min})})}} \\ & \times \left[T_{mean} - \left(-2.5 - 0.14\left(e_{s(T_{max})} - e_{s(T_{min})}\right) - \frac{Elevat}{550}\right)\right] R_a \end{aligned} \tag{A3}$$

   where $Elevat$ is the altitude (m), $e_{s(T_{min})}$ is the saturation vapor pressure (kPa) at the minimum temperature, $e_{s(T_{max})}$ is the saturation vapor pressure (kPa) at the maximum temperature, $e_{a(T_{min})}$ is the actual vapor pressure (kPa) at the minimum temperature, and $e_{a(T_{max})}$ is the actual vapor pressure (kPa) at the maximum temperature. This method is known to overestimate ET_0 in humid areas and underestimate it in arid and semi-arid regions.
4. Linacre
   The Linacre method can be written as follows:

$$ET_0 = \frac{\frac{700(T_{mean} + 0.0006Z)}{100 - L} + 15(T_{mean} - T_d)}{80 - T_{mean}} \tag{A4}$$

   where Z is altitude (m), L is latitude in the degree, and T_d is the dew point.

5. Turc
Finally, the Turc method can be written as follows:

$$\begin{aligned} PET &= 0.013\left(\frac{T_{mean}}{15+T_{mean}}\right)(R_s+50), \qquad RH > 50\% \\ &= 0.013\left(\frac{T_{mean}}{15+T_{mean}}\right)(R_s+50)\left(1+\frac{50-RH}{70}\right), \qquad RH < 50\% \end{aligned} \tag{A5}$$

where R_s is the mean solar radiation(W/m^{2}day) and RH is the relative humidity(%).

Appendix B. Maximum Likelihood Estimation (MLE)

Maximum likelihood estimation is a common statistical method used to estimate the parameters of a statistical model. Conditional maximum likelihood estimation (CMLE) is a type of MLE that takes into account the presence of conditional information in the data. In CMLE, the likelihood function is maximized with respect to the model parameters under the condition that certain variables in the model are held constant. We define our conditional likelihood function as

$$L(\mu, \lambda, \hat{\gamma}) = \prod_{t=1}^{n} f(X_t | X_{t-1}; \mu, \lambda, \hat{\gamma}). \tag{A6}$$

Applying the conditional maximum likelihood estimation to the solution of the SDE, the conditional probability function of X_t given X_{t-1} is given by

$$f(X_t | X_{t-1}; \mu, \lambda, \hat{\gamma}) = \frac{1}{\sqrt{2\pi\hat{\gamma}^2}} \exp\left[-\frac{\left(X_t - X_{t-1}e^{-\lambda\delta} - \mu\left(1-e^{-\lambda\delta}\right)\right)^2}{2\hat{\gamma}^2}\right], \tag{A7}$$

$$\hat{\gamma}^2 = \gamma^2 \frac{1-e^{-2\lambda\delta}}{2\lambda}. \tag{A8}$$

The log-likelihood function is derived from the conditional probability function,

$$\begin{aligned} l(\mu, \lambda, \hat{\gamma}) &= \sum_{t=1}^{n} \ln f(X_t | X_{t-1}; \mu, \lambda, \hat{\gamma}) \\ &= -\frac{n}{2}\ln 2\pi - n\ln\hat{\gamma} - \frac{1}{2\hat{\gamma}^2}\sum_{t=1}^{n}\left[X_t - X_{t-1}e^{-\lambda\delta} - \mu\left(1-e^{-\lambda\delta}\right)\right]^2. \end{aligned} \tag{A9}$$

The maximum likelihood estimator has a value that is satisfied when all partial derivatives (with respect to each parameter) are zero. Partial derivatives with respect to each parameter and solution are presented below.

$$\frac{\partial l(\mu, \lambda, \hat{\gamma})}{\partial \mu} = \frac{1}{\hat{\gamma}^2}\sum_{t=1}^{n}\left[X_t - X_{t-1}e^{-\lambda\delta} - \mu\left(1-e^{\lambda\delta}\right)\right](1-e^{-\lambda\delta}) = 0, \tag{A10}$$

$$\mu = \frac{\sum_{t=1}^{n}\left[X_t - X_{t-1}e^{-\lambda\delta}\right]}{n(1-e^{-\lambda\delta})}, \tag{A11}$$

$$\frac{\partial l(\mu, \lambda, \hat{\gamma})}{\partial \lambda} = -\frac{\delta e^{-\lambda\delta}}{\hat{\gamma}^2}\sum_{t=1}^{n}\left[(X_t-\mu)(X_{t-1}-\mu) - e^{-\lambda\delta}(X_{t-1}-\mu)^2\right] = 0, \tag{A12}$$

$$\lambda = -\frac{1}{\delta}\ln\frac{\sum_{t=1}^{n}(X_t-\mu)(X_{t-1}-\mu)}{\sum_{t=1}^{n}(X_{t-1}-\mu)^2}, \tag{A13}$$

$$\frac{\partial l(\mu,\lambda,\hat{\gamma})}{\partial \hat{\gamma}} = -\frac{n}{\hat{\gamma}} + \frac{1}{\hat{\gamma}^3}\sum_{t=1}^{n}\left[X_t - X_{t-1}e^{-\lambda\delta} - \mu(1-e^{-\lambda\delta})\right] = 0\,, \tag{A14}$$

$$\hat{\gamma}^2 = \frac{1}{n}\sum_{t=1}^{n}\left[X_t - X_{t-1}e^{-\lambda\delta} - \mu\left(1-e^{-\lambda\delta}\right)\right]^2. \tag{A15}$$

Note that the solutions of μ and λ are dependent on each other. The solution of μ is affected by λ; likewise, λ is affected by μ. Therefore, at least knowing one value of these two parameters is required to find μ and λ. In order to overcome this problem, a substitution of λ into μ is applied. Once μ and λ are determined, γ can be found. Therefore, the parameters are given as follows.

$$\mu = \frac{S_y - e^{-\lambda\delta}S_x}{n(1-e^{-\lambda\delta})}\,, \tag{A16}$$

$$\mu = \frac{S_yS_{xx} - S_xS_{xy}}{n(S_{xx}-S_{xy})({S_x}^2 - S_xS_y)}\,, \tag{A17}$$

$$\lambda = -\frac{1}{\delta}\ln\frac{S_{xy} - \mu S_x - \mu S_y + n\mu^2}{S_{xx} - 2\mu S_x + n\mu^2}\,, \tag{A18}$$

$$\begin{aligned}\hat{\gamma}^2 = \frac{1}{n}[&S_{yy} - 2e^{-\lambda\delta}S_{xy} + e^{-2\lambda\delta}S_{xx}\\ &- 2\mu(1-e^{-\lambda\delta})(S_y - e^{-\lambda\delta}S_x) + n\mu^2(1-e^{-\lambda\delta})^2]\,,\end{aligned} \tag{A19}$$

$$\gamma^2 = \hat{\gamma}^2\frac{2\lambda}{1-e^{-2\lambda\delta}}\,. \tag{A20}$$

References

1. Zhu, J.; Pollanen, M.; Abdella, K.; Cater, B. Modeling Drought Option Contracts. *ISRN Appl. Math.* **2012**, *2012*, 251835. [CrossRef]
2. Alexandridis, K.A.; Zapranis, A.D. *Weather Derivatives: Modeling and Pricing Weather-Related Risk*; Springer: New York, NY, USA, 2013.
3. Dischel, B. Shaping history for weather risk management. *Energy Power Risk* **1999**, *12*, 13–15.
4. Dorfleitner, G.; Wimmer, M. The pricing of temperature futures at the Chicago Mercantile Exchange. *J. Bank Financ.* **2010**, *34*, 1360–1370. [CrossRef]
5. Jewson, S.; Brix, A.; Ziehmann, C. *Weather Derivative Valuation: The Meteorological, Statistical, Financial and Mathematical Foundations*; Cambridge University Press: Cambridge, UK, 2005.
6. Brody, D.; Syroka, J.; Zervos, M. Dynamical pricing of weather derivatives. *Quant. Financ.* **2002**, *2*, 189–198. [CrossRef]
7. Richards, T.J.; Manfredo, M.R.; Sanders, D.R. Pricing weather derivatives. *Am. J. Agric. Econ.* **2004**, *86*, 1005–1017. [CrossRef]
8. Geman, H.; Leonardi, M. Alternative approaches to weather derivatives pricing. *Manag. Financ.* **2005**, *31*, 46–72. [CrossRef]
9. Taylor, J.W.; Buizza, R. A comparison of temperature density forecasts from GARCH and atmospheric models. *J. Forecast.* **2004**, *23*, 337–355. [CrossRef]
10. Carmona, R. Calibrating degree day options. In Proceedings of the 3rd Seminar on Stochastic Analysis, Random Field and Applications, École Polytechnique de Lausanne, Ascona, Switzerland, 23 September 1999.
11. Cao, M.; Wei, J. Pricing the weather. *Risk* **2000**, *13*, 67–70.
12. McIntyre, R.; Doherty, S. Weather Risk—An example from the UK. *Energy Power Risk Manag.* **1999**.
13. Dornier, F.; Queruel, M. Caution to the wind. Weather risk special report. *Energy Power Risk Manag.* **2000**, *13*, 30–32.
14. Bhowan, A. Temperature Derivatives. Ph.D. Thesis, University of Wiwatersand, Johannesburg, South Africa, 2003.
15. Williams, C.B. Sequences of wet and of dry days considered in relation to the logarithmic series. *Q. J. R. Meteorol. Soc.* **1952**, *78*, 91–96. [CrossRef]
16. Longley, R. W. The length of dry and wet periods. *Q. J. R. Meteorol. Soc.* **1953**, *79*, 520–527. [CrossRef]
17. Chin, E.H. Modeling daily precipitation occurrence process with Markov chain. *Water Resour. Res.* **1977**, *13*, 949–956. [CrossRef]
18. Richardson, C.W. Stochastic simulation of daily precipitation, temperature, and solar radiation. *Water Resour. Res.* **1981**, *17*, 182–190. [CrossRef]
19. Wilks, D.S. Interannual variability and extreme-value characteristics of several stochastic daily precipitation models. *Agric. For. Meteorol.* **1999**, *93*, 153–169. [CrossRef]
20. Dennett, M.D.J.; Rodgers, J.A.; Keatinge, J.D.H. Simulation of a rainfall record for a new site of a new agricultural development: an example from northern Syria. *Agric. Meteorol.* **1983**, *29*, 247–258. [CrossRef]

21. Jones, P.G.; Thornton, P.K. Spatial and temporal variability of rainfall related to a third-order Markov model. *Agric. For. Meteorol.* **1997**, *86*, 127–138. [CrossRef]
22. Göncü, A. Modeling and pricing precipitation-based weather derivatives. *Financ. Math. Appl.* **2011**, *1*, 9–18.
23. Tsakiris, G.; Pangalou, D.; Vangelis, H. Regional drought assessment based on the Reconnaissance Drought Index (RDI). *Water Resour. Manag.* **2007**, *21*, 821–833. [CrossRef]
24. Allen, R.G.; Pereira, L.S.; Raes, D.; Smith, M. *Crop Evapotranspiration-Guidelines for Computing Crop Water Requirements-FAO*; Irrigation and Drainage Paper 56; Food and Agriculture Organization of the United Nations: Rome, Italy, 1998.
25. Allen, R.; Pruitt W. O. Rational Use of The FAO Blaney-Criddle Formula. *J. Irrig. Drain. Eng.-ASCE* **1986**, *112*, 139–155. [CrossRef]
26. Hargreaves, G.H.; Samani, Z.A. Reference Crop Evapotranspiration from Temperature. *Appl. Eng. Agric.* **1985**, *1*, 96–99. [CrossRef]
27. Jensen, M.E.; Haise, H.R. Estimating Evapotranspiration from Solar Radiation. *Proc. Am. Soc. Civ. Eng. J. Irrig. Drain. Div.* **1963**, *89*, 15–41. [CrossRef]
28. Linacre, E.T. A Simple Formula for Estimating Evaporation Rates in Various Climates, using Temperature Data Alone. *Agricult. Meteorol.* **1977**, *1*, 409–424. [CrossRef]
29. Turc, L. Estimation of irrigation water requirements, potential evapotranspiration: A simple climatic formula evolved up to date. *Ann. Agron.* **1961**, *12*, 13–49.
30. Van den Berg, T. Calibrating the Ornstein-Uhlenbeck (Vasicek) Model. Available online: https://www.statisticshowto.datasciencecentral.com/wp-content/uploads/2016/01/Calibrating-the-Ornstein.pdf. (accessed on 8 March 2023).
31. Gabriel, K.R.; Neumann, J. A Markov chain model for daily rainfall occurrence at Tel Aviv. *Q. J. R. Meteorol. Soc.* **1962**, *88*, 90–95. [CrossRef]
32. Katz, R.W. Computing probabilities associated with the Markov chain model for precipitation. *J. Appl. Meteorol. Climatol.* **1974**, *13*, 953–954. [CrossRef]
33. Hui, W.; Xuebin, Z.; Elaine, M.B. Stochastic Modeling of Daily precipitation for Canada. *Atmospheric* **2005**, *43*, 23–32.
34. Hosking, J.R.M. The four-parameter Kappa distribution. *IBM J. Res. Dev.t* **1994**, *38*, 251–258. [CrossRef]
35. Akaike, H. A new look at the statistical model identification. *IEEE Trans. Autom. Control.* **1974**, *19*, 716–723.
36. Schwarz, G. Estimating the Dimension of a Model. *Ann. Stat.* **1978**, *6*, 461–464. [CrossRef]